

# Characterization of zone plate properties using monochromatic synchrotron radiation in the 2 to 20 nm wavelength range

John Seely,<sup>1,\*</sup> Benjawan Kjornrattanawanich,<sup>2,3</sup> Leonid Goray,<sup>4,5</sup>  
Yan Feng,<sup>6</sup> and James Bremer<sup>7</sup>

<sup>1</sup>Naval Research Laboratory, 4555 Overlook Avenue SW, Washington, DC 20375, USA

<sup>2</sup>Artep Inc., 2922 Excelsior Springs Court, Ellicott City, Maryland 21042, USA

<sup>3</sup>National Synchrotron Light Source Beamline X24C, Brookhaven National Laboratory, Upton, New York 11973, USA

<sup>4</sup>St Petersburg Academic University, Russian Academy of Sciences, 8/3 Khlopina Street, St. Petersburg 194021, Russia

<sup>5</sup>Institute for Analytical Instrumentation, Russian Academy of Sciences, Rizhsky Pr. 26, St. Petersburg 190103, Russia

<sup>6</sup>Xradia Inc., 4385 Hopyard Road, Pleasanton, California 94588, USA

<sup>7</sup>Research Support Instruments Inc., 4325-B Forbes Blvd., Lanham, Maryland 20706, USA

\*Corresponding author: john.seely@nrl.navy.mil

Received 18 April 2011; revised 18 May 2011; accepted 23 May 2011;  
posted 23 May 2011 (Doc. ID 145598); published 15 June 2011

A zone plate composed of Mo zones having 4 mm outermost zone diameter, 100 nm outermost zone width, and supported on a silicon nitride membrane was characterized using monochromatic synchrotron radiation in the 2 to 20 nm wavelength range. The zero and first order efficiencies were measured and compared to *ab initio* calculations that account for the optical properties of the materials, the width and shape of the zones, and multiple-layer thin-film effects. It is shown that the thicknesses of the Mo zones and the membrane and the ratio of the zone width to zone period can be independently determined from the measured diffraction efficiencies in the zero and first orders and that the computational code can be used to reliably design zone plates that are optimized for applications such as solar irradiance monitors in the extreme ultraviolet region.

OCIS codes: 050.1950, 050.1960, 340.7480.

## 1. Introduction

Zone plates have been widely used for microscopy and microlithography in wavelength regions from the visible to soft x-rays, most recently at 13 nm wavelength in the extreme ultraviolet (EUV) region [1]. Zone plates have been proposed for spaceflight instrumentation that accurately measures the EUV emission from the sun at wavelengths up to 100 nm [2–4]. When optimizing a zone plate (ZP) design for particular EUV applications, it is necessary to characterize the optical performance of the ZP, thoroughly understand the physical dimensions such as the thicknesses of the zones and the supporting

membrane to nm accuracy, determine the effects of zone and membrane transmittance on the diffraction efficiency, and computationally model the efficiency. We describe techniques for accurately measuring the ZP optical performance using monochromatic synchrotron radiation over a wide wavelength range, from 2 to 20 nm, and for determining the ZP properties by comparisons with *ab initio* calculations of the diffraction efficiencies in the zero and first orders.

The diffraction of radiation by a ZP is shown schematically in Fig. 1. The circular zones fill the space  $Z$  between the central occulter  $C$  and outer occulter  $O$ . The radiation is incident from the left, and the zero diffraction order 0 passes undeflected through the

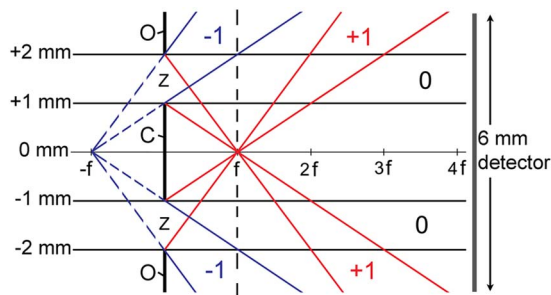


Fig. 1. (Color online) Schematic of the central occulter  $C$  having 1 mm radius, the outer occulter  $O$  having 2 mm radius opening, and the zones  $Z$  filling the space between the central and outer occulters. The radiation is incident from the left, and indicated are the undeflected zero order (0), focused first order (+1), and diverging first order (-1). Also indicated is the detector with 6 mm diameter aperture.

zones. The converging first order (+1) passes through the focal point at a distance  $f$  from the zones, and the diverging first order (-1) appears to originate from a virtual source at  $-f$ . The focal distance  $f$  is equal to  $\Delta r_N D / m \lambda$ , where  $\Delta r_N$  is the width of the outermost zone,  $D$  is the diameter of the outermost zone,  $m$  is the diffraction order number, and  $\lambda$  is the wavelength of the incident radiation [1]. Thus the higher  $+m$  orders are focused closer to the ZP and the higher  $-m$  orders have larger divergence angles from the zones.

While the +1 converging order is typically utilized in a specific wavelength range for most applications, it is important to measure the efficiencies in other orders for a more complete understanding of the ZP performance and the physical properties that influence performance such as zone and membrane thicknesses. In addition, in the case of broadband illumination of the ZP, out-of band radiation can adversely affect the in-band performance at the selected wavelength. This is particularly important for solar radiometers that are illuminated by bright radiation from a source  $>0.5^\circ$  in diameter spanning the wavelength range from x-ray through visible.

The +1 efficiency of a ZP having Mo zones with 100 nm outermost zone width and 4 mm diameter was calibrated in the 7 to 18 nm wavelength range using monochromatic synchrotron radiation [4]. The manufacturing specifications indicated the Mo zones were 70 nm thick, and the zones were mounted on a  $\text{Si}_3\text{N}_4$  support membrane having nominal 100 nm thickness and a much thinner Ti interface layer of 5 nm thickness. We discuss here the measurement of the zero order efficiency over the extended wavelength range 2 to 20 nm and comparisons with *ab initio* efficiency calculations that enable an accurate determination of the ZP structure.

The primary motivation for this work is to understand the roles of zone and membrane transmittances on the efficiencies and possible thin-film effects resulting from the multiple-layer structure of the ZP. Such understanding is required when designing future zone plates for solar radiometer applications in the longer wavelength EUV region

(up to 100 nm) where multiple-layer interference effects can become important.

## 2. Efficiency measurements

The efficiency measurements were performed at the Naval Research Laboratory beamline X24C at the National Synchrotron Light Source at Brookhaven National Laboratory. The 600 groove/mm grating in the beamline monochromator provided a practically monochromatic beam (400 resolving power) to the calibration chamber. The ZP was mounted on a goniometer (providing tip and roll motions) and on a rotational stage (providing yaw motion), and this assembly was mounted on an  $x$ - $y$  translation stage. The ZP could be accurately translated into the radiation beam and rotated about orthogonal axes with respect to the beam under computer control. The divergence of the radiation beam from the monochromator was typically 0.6 mrad, and the beam size could be varied over the range 0.5 to 4 mm by changing the beamline apertures and baffles. Thin filters were inserted into the beam to pass the wavelength region of interest while attenuating higher harmonic radiation from the monochromator grating at shorter wavelengths.

A detector assembly was positioned behind the ZP and was mounted on an  $x$ - $y$ - $z$  translation stage, and a selected detector could be accurately moved with respect to the ZP under computer control. Mounted on the detector assembly were silicon photodiode detectors (type AXUV100G from International Radiation Detectors Inc.) with 0.15 mm, 0.40 mm, and 6 mm diameter apertures. Also mounted on the detector assembly were a complementary metal oxide semiconductor (CMOS) imager having  $48 \mu\text{m}$  pixel size and a CCD imager having  $5.2 \mu\text{m}$  pixel size. The imagers had phosphor coatings for EUV sensitivity.

When measuring the ZP efficiency, it is first necessary to record and understand the diffraction pattern of the converging and diverging low orders, at least the zero and first orders, with an imaging detector. Then a photodiode detector with a small aperture can be positioned to accurately measure the efficiency of a selected order, uncontaminated by radiation from other orders.

The diffraction patterns were recorded by positioning the CMOS or CCD imager at the focal distance of the first orders of a number of selected incident wavelengths as indicated by the dashed vertical line in Fig. 1. The diffraction pattern of 15.6 nm radiation, at its +1 order focal plane, recorded by the CMOS imager is shown in Fig. 2. The 0 order radiation passes undeflected through the zones and casts a shadow of the 2 mm outside diameter (OD) central occulter, including the four support spokes, and of the 4 mm inside diameter (ID) outer occulter. Also visible are the focused +1 order and the diverging -1 order including the  $2\times$  magnified shadow of the four support spokes. The 0 and +1 order rays fall within the  $2\times$  shadow of the central occulter and are therefore separated from the diverging -1 order rays. In

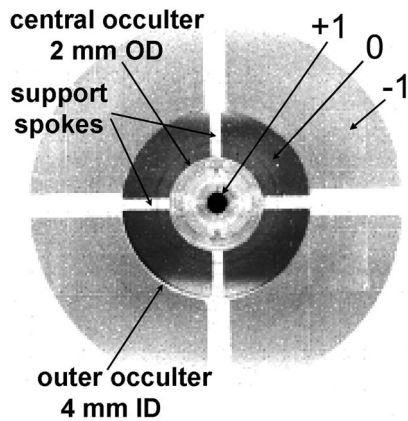


Fig. 2. Image of the diffraction pattern of 15.6 nm radiation where the zero order (0), focused first order (+1), and diverging first order (-1) are identified.

addition, the diverging rays of the -1 order fall in the shadow of the outer occulter and are separated from the 0 order rays. This beneficial separation of diffraction orders occurs when the ID of the outer occulter is no more than twice the OD of the central occulter.

The metrology provided by the CMOS and CCD imagers was used to accurately scan an apertured photodiode through the diffraction pattern of a selected wavelength. For example, as indicated in Fig. 1, the photodiode with a 6 mm diameter aperture collects only the 0 order when at a distance  $>4f$  from the ZP. When moved toward the ZP, the photodiode begins to collect the +1 order radiation at a  $4f$  distance from the ZP and collects all of the +1 order at distances  $<2.5f$ . The photodiode also collects, in sequence, the -1 order beginning at a distance of  $2f$  and the higher orders. Shown by the data points in Fig. 3(a) are the efficiencies measured by scanning the apertured photodiode toward the ZP when illuminated by 18.5 nm radiation. The curves are the efficiencies calculated as described in Section 3 and using the ZP and detector geometries, and in addition assuming uniform illumination of the zones. The curve for total calculated efficiency is in good agreement with the data points except near the cusp at distance  $f = 2.5$ , and this disagreement results from the slightly nonuniform incident beam near the ID of the outer occulter (see Fig. 2). Shown in Fig. 3(b) are the efficiencies of an ideal Fresnel ZP having opaque zones and transparent open spaces between the zones, where the zero order efficiency is 25%, the odd order efficiencies are  $1/(m\pi)^2$ , and the even order efficiencies are zero [1]. It is immediately obvious that the Mo ZP has nonideal efficiency resulting from partially transmitting zones and a partially transmitting support membrane.

In order to fully characterize and understand the ZP efficiency, including the role of zone and membrane transmittance, it is necessary to accurately measure the efficiency over a wide wavelength range covering the attenuation edges and other features of the elements in the zones and membrane. This is conveniently done for the 0 order by positioning the

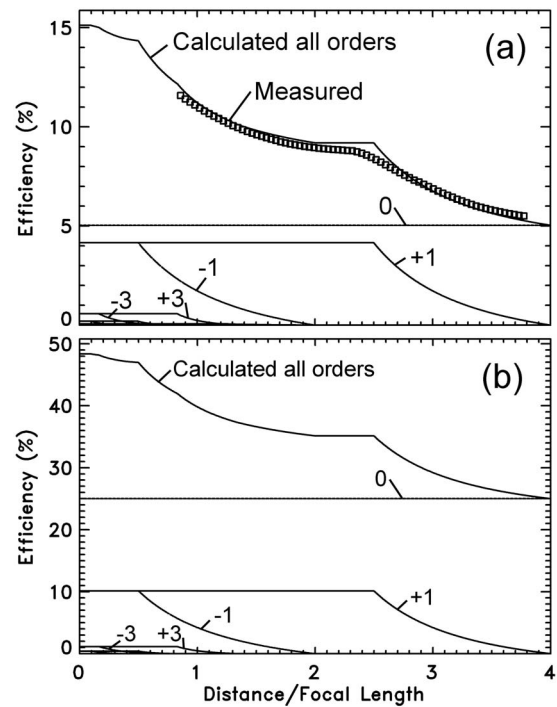


Fig. 3. (a) Comparison of the 18.5 nm efficiency of the Mo ZP measured by the 6 mm detector when scanned in distance with respect to the ZP (data points) and the calculated efficiency curves. (b) Efficiency curves for an ideal Fresnel ZP.

detector far from the ZP where it collects only the undeflected 0 order and scanning the wavelength of the incident radiation using the beamline monochromator. The measured 0 order efficiency is shown by the thick curve in Fig. 4, and many spectral features are present that enable the accurate determination of the transmittances and thicknesses of the Mo zones and the  $\text{Si}_3\text{N}_4$  support membrane. Notable in the 0 order efficiency curve are the Si  $L_3$  attenuation edge at 12.4 nm, the N K edge at 3.1 nm, and the Mo M edge near 5 nm.

Owing to the converging and diverging nature of the higher orders, when measuring the efficiency

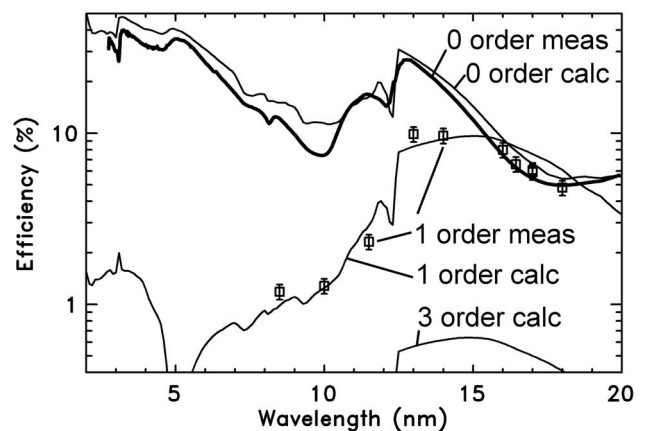


Fig. 4. Comparison of the measured 0 order efficiency (thick curve) and +1 order efficiency (square data symbols) with the calculated efficiencies.

of a selected converging order a detector with a small aperture must be positioned at the focus of the selected order so that rays from only the selected order are collected. Since the focal length varies inversely with wavelength, the small aperture must be scanned in  $z$ , the distance between the aperture and the ZP, to maximize the signal at the focal distance. In addition, the small aperture must be centered laterally in  $x$  and  $y$ . The square data points in Fig. 4 are such measurements of the +1 order. It was verified that the -1 order has the same efficiency (within the accuracy of the measurements) as the +1 order using the  $z$  scanning technique of Fig. 3 and the CMOS images of Fig. 2.

We note that when positioning the small apertured detector at the focal distance of the +1 order,  $f = 1$  in Fig. 3, a small contribution from the +3 order can pass through the aperture and add to the +1 order signal. However, the +3 order contribution is much lower than the +1 order signal and was not noticeable when scanning the apertured detector in  $z$  through the +1 order focal distance. Thus the +3 order contribution was neglected.

### 3. Calculated efficiencies

The thin curves in Fig. 4 are the efficiencies calculated using the PCGRATE code [5]. This code is based on the rigorous boundary integral equation method [6] and calculates the diffraction efficiency of electromagnetic waves incident on transmitting (and reflecting) periodic and/or nonperiodic structures having realistic physical configurations and multiple material layers. The high accuracy of the code's calculated efficiencies of reflection gratings having multilayer coatings and operating in the soft x-ray-EUV region has been verified [6–8]. Our first attempt to calculate the transmittance of ZP structures using the rigorous electromagnetic code was undertaken in [3]. All widely used approaches that are based on the scalar theory of diffraction (the high-frequency Kirchoff integral approximation) have a fundamental constraint on their application to bulk and multilayer x-ray-EUV structures having line parameters (period, outermost zone width, correlation length) comparable to the working wavelength. The limitation is connected with the difference in scattering between the finitely and perfectly conducting surfaces.

The ZP was modeled using three layers, the Mo zones and a  $\text{Si}_3\text{N}_4$  support membrane having a 5 nm Ti intermediate layer as illustrated in Fig. 5. The Mo zones, Ti intermediate layer, and  $\text{Si}_3\text{N}_4$  membrane have thicknesses of  $t_{\text{Mo}}$ ,  $t_{\text{Ti}}$ , and  $t_m$ , respectively. The period width is  $p$ , the open space between Mo zones has width  $o$ , and the Mo zone width is  $p - o$ . The optical constants were derived from the tabulated optical constants of the elements and assuming bulk density [9].

Simple analytical expressions for the ZP efficiency were initially used to obtain values for the zone thickness and width [10]. These expressions account

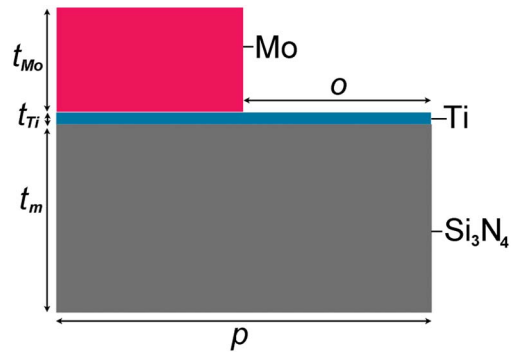


Fig. 5. (Color online) Schematic of the ZP consisting of Mo zones and  $\text{Si}_3\text{N}_4$  support membrane and a Ti intermediate layer.

for the thickness, width, and transmittance of the zones but not the  $\text{Si}_3\text{N}_4$  membrane and Ti intermediate layer. In this approximation, the ratio of the first and zero order efficiencies is independent of the membrane transmittance and depends only on the zone thickness and open space to period width,  $t_{\text{Mo}}$  and  $o/p$  in Fig. 5. Shown in Fig. 6(a) is the first to zero order efficiency ratio calculated by assuming the ideal  $o/p$  ratio 0.5 and varying the Mo zone thickness. For wavelengths  $< 15$  nm, the best agreement with the measure efficiency ratio occurs at 45 nm zone thickness with an uncertainty of  $\pm 5$  nm; the

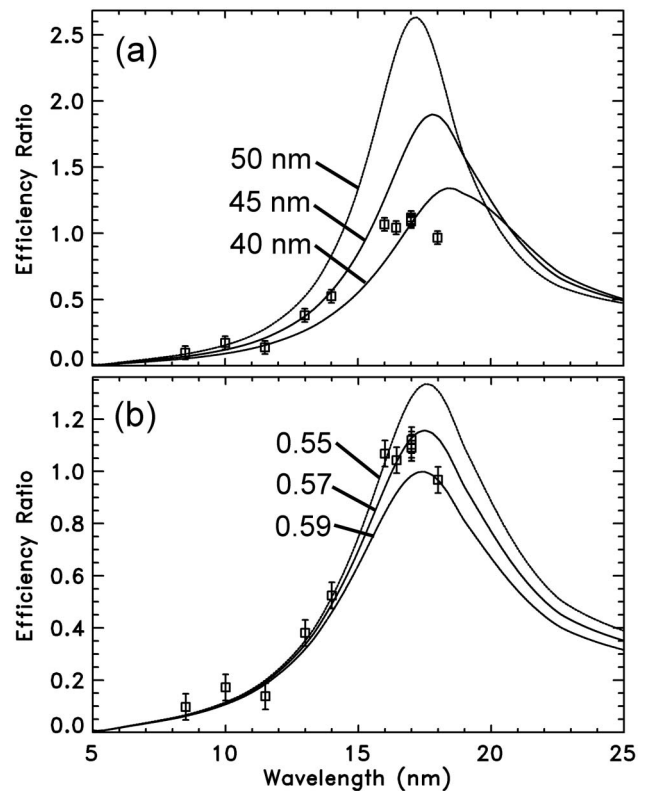


Fig. 6. The curves are the ratios of the calculated first and zero order efficiencies, and the data symbols are the measured ratios. (a) Calculated for fixed open space to period ratio 0.50 and for Mo zone thicknesses of 50 nm, 45 nm, and 40 nm. (b) Calculated for fixed 45 nm Mo zone thickness and open space to period ratios of 0.55, 0.57, and 0.59.

efficiency ratio is highly sensitive to zone thickness for wavelengths  $>15$  nm. We note that inaccurate Mo optical constants can affect the inferred Mo thickness; for example increasing the attenuation coefficient would reduce the inferred Mo thickness.

Assuming 45 nm zone thickness, the efficiency ratio was calculated for variable  $o/p$  and is shown in Fig. 6(b). The efficiency ratio is insensitive to  $o/p$  for wavelengths  $<15$  nm and is highly sensitive for wavelengths  $>15$  nm where 0.57 gives the best agreement with the measurements with an uncertainty of  $\pm 0.02$ . Thus we infer the Mo zone thickness (45 nm) and the zone width (0.43 of the zone period) independently from the efficiency ratios in the  $<15$  nm and  $>15$  nm wavelength regions, respectively.

Shown in Fig. 7 is a comparison of the ratio of the +1 and 0 order efficiencies calculated by the analytical expressions (curve 1) and by the PCGRATE code (curve 2) using the same 45 nm Mo zone thickness and  $o/p = 0.57$  parameters and using the same Mo optical constants. The ratios exactly agree at  $<10$  nm wavelengths and have disagreements at longer wavelengths. The origin of these disagreements will require additional measurements and calculations to understand and will be the subject of future research. It is possible that the disagreements result from multiple-layer thin-film effects that are known to occur in the EUV region [11].

The absolute efficiency values of the multiple-layer ZP as illustrated in Fig. 5 were calculated using the PCGRATE code, and the thickness of the  $\text{Si}_3\text{N}_4$  membrane was varied to achieve the best agreement with the measured first and zero order efficiencies. Fixed parameters were the Mo zone thickness (45 nm), the open space to period ratio ( $o/p = 0.57$ ), and the Ti layer thickness (5 nm). In addition, the zones were assumed to have the ideal rectangular shape of Fig. 5. When varying the membrane thickness, it was found that the jumps in the 0 order efficiency curve near the 12.4 nm Si  $L_3$  and 3.1 nm N K edges were quite sensitive to the assumed membrane thickness.

The best overall agreement between the first and zero order calculated and measured efficiencies

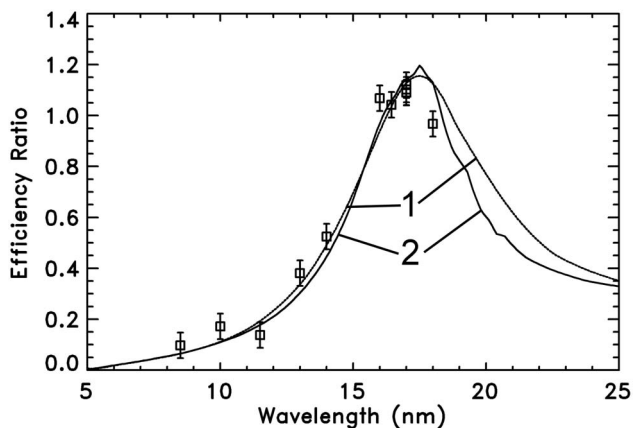


Fig. 7. The ratios of the first and zero order efficiencies calculated using the analytical expressions (curve 1) and the PCGRATE code (curve 2). The data symbols are the measured ratios.

occurred for 70 nm  $\text{Si}_3\text{N}_4$  membrane thickness and is shown by the thin curves in Fig. 4. There are significant differences between the calculated and measured efficiencies. These differences could not be substantially reduced by varying the other ZP parameters. For example, the calculated efficiencies were insensitive to the zone period, which changes continuously from 400 nm at the central occulter to 200 nm at the outer occulter, and to reasonable changes to the shape of the Mo zones. Changes to the Ti layer, with nominal thickness of 5 nm, had small effect on the calculated efficiencies owing to the thinness of the Ti layer compared to the Mo zones and the membrane. Finally, altering the Mo thickness and width from the values 45 nm and  $o/p = 0.57$  adversely affect the good agreement with the measured +1 to 0 order efficiency ratio shown in Fig. 7 (curve 2).

The most likely cause of the disagreement between the calculated and measured efficiencies is inaccurate optical constants for the Mo zones and  $\text{Si}_3\text{N}_4$  membrane (the Ti intermediate layer is too thin to significantly affect the efficiencies). It is well known that Mo films can oxidize and form compounds with neighboring materials, and the chemical composition and surface conditions of the membrane can also vary from the ideal  $\text{Si}_3\text{N}_4$ . Thus the optical constants derived from the elements Mo, Si, and N for the zones and membrane can be inaccurate, particularly at the longer EUV wavelengths where molecular effects can influence optical performance [12]. Moreover, the inferred zone and membrane thicknesses, 45 nm and 70 nm, are much smaller than the values expected from the design of the ZP, 70 nm and 100 nm, respectively, and this is further evidence of inaccurate zone and membrane EUV optical properties used in the calculations.

#### 4. Conclusions

A number of techniques have been utilized for experimentally characterizing zone plates in the EUV wavelength region using monochromatic synchrotron radiation: determining the efficiencies of the converging  $+m$  and diverging  $-m$  orders from the diffraction pattern recorded by CMOS and CCD imagers, measuring the spectrum of the 0 order efficiency over a wide wavelength range by positioning the large area detector far from the ZP, scanning the detector toward the ZP and collecting in sequence the higher  $+m$  and  $-m$  orders, and measuring the efficiency of a converging order by accurately positioning a detector with a small aperture at the focal position. These different techniques provide redundancies that enable the accurate measurement of the efficiencies of all the strongest orders.

The techniques were utilized to measure the efficiencies of a ZP consisting of partially transmitting Mo zones and  $\text{Si}_3\text{N}_4$  support membrane, and the material thicknesses were inferred by comparing to the calculated efficiencies. As has been demonstrated for reflection gratings having thin-film multilayer

coatings and operating in the EUV region [7,8], the realistic ZP modeling and accurate calculation of EUV efficiencies have the potential of providing practical guidance for the design and optimization of ZPs for spaceflight EUV instrumentation. However, significant difference exists between the calculated and measured ZP efficiencies, most likely resulting from inaccurate optical properties of the zone and membrane materials, and this illustrates the importance of accurately measuring the optical properties and efficiencies using synchrotron radiation and of improving the accuracy of the ZP computational modeling.

This work was supported by the NASA project Ultra-Stable Extreme Ultraviolet Solar Monitor using Zone Plates and by the Office of Naval Research (ONR).

## References

1. David Attwood, *Soft X-Rays and Extreme Ultraviolet Radiation* (Cambridge University Press, 2000), pp. 337–394.
2. J. C. Bremer and W. Yun, “Concept for an extreme ultraviolet sensor with a Fresnel zone plate for the GOES-R Solar Imaging Suite,” *Proc. SPIE* **5901**, 59010P-1–59010P-12 (2005).
3. J. Seely, G. Holland, J. Bremer, T. Zukowski, M. Feser, Y. Feng, B. Kjørnattawanich, and L. Goray, “Measurement of zone plate efficiencies in the extreme ultraviolet and applications to radiation monitors for absolute spectral emission,” *Proc. SPIE* **6317**, 63170N-1–63170N-8 (2006).
4. J. Seely, B. Kjørnattawanich, J. Bremer, M. Kowalski, and Y. Feng, “Radiometry and metrology of a zone plate measured by extreme ultraviolet synchrotron radiation,” *Appl. Opt.* **48**, 5970–5977 (2009).
5. International Intellectual Group Inc., <http://pcgrate.com/>.
6. L. I. Goray, J. F. Seely, and S. Yu. Sadov, “Spectral separation of the efficiencies of the inside and outside orders of soft-x-ray–extreme-ultraviolet gratings at near normal incidence,” *J. Appl. Phys.* **100**, 094901-1–094901-13 (2006).
7. L. Goray and J. Seely, “Efficiencies of master, replica, and multilayer gratings for the soft x-ray–extreme ultraviolet range: modeling based on the modified integral method and comparisons with measurements,” *Appl. Opt.* **41**, 1434–1445 (2002).
8. J. Seely, C. Brown, D. Windt, S. Donguy, and B. Kjørnattawanich, “Normal-incidence efficiencies of multilayer-coated laminar gratings for the Extreme-Ultraviolet Imaging Spectrometer (EIS) on the Solar-B Mission,” *Appl. Opt.* **43**, 1463–1471 (2004).
9. Center for X-Ray Optics, <http://www.cxro.lbl.gov/>.
10. H. W. Schnopper, L. P. Van Speybroeck, J. P. Delvaille, A. Epstein, E. Källne, R. Z. Bachrach, J. Dijkstra, and L. Lantward, “Diffraction Grating Transmission Efficiencies for XUV and Soft X Rays,” *Appl. Opt.* **16**, 1088–1091 (1977).
11. J. F. Seely, “Extreme-Ultraviolet Thin-Film Interference in an Al-Mg-Al Multiple-layer Transmission Filter,” *Appl. Opt.* **41**, 5979–5983 (2002).
12. J. F. Seely, L. I. Goray, D. L. Windt, Yu. A. Uspenskii, A. V. Vinogradov, and B. Kjørnattawanich, “Extreme ultraviolet optical constants for the design and fabrication of multilayer gratings,” *Proc. SPIE* **5538**, 43–53 (2004).